

Effect of seed layers in improving the crystallographic texture of CoCrPt perpendicular recording media

Anup G. Roy^{a)}

Data Storage Systems Center, Electrical and Computer Engineering Department, Carnegie Mellon University, Pittsburgh, Pennsylvania 15213-3890.

David E. Laughlin

Data Storage Systems Center, Department of Materials Science and Engineering, Carnegie Mellon University, Pittsburgh, Pennsylvania 15213-3890

In this work, we have systematically investigated the effect of Ti and Ta seed layers on the improvement of *c*-axis alignment of the CoCrPt film. We studied the film texture by x-ray diffraction and electron diffraction, and microstructure and morphology by high-resolution transmission electron microscopy. Both Ti and Ta improve the texture of CoCrPt perpendicular magnetic media depending on the seed layer thickness. The 5–10-nm thick seed layer shows the best *c*-axis alignment of CoCrPt films when the seed layer is amorphous. The *c*-axis alignment of magnetic layer deteriorates for random texture and mixed amorphous and crystalline microstructure of the seed layer. The texture of the magnetic layer improves for the film with about 40-nm-thick seed layer with the development of favorable texture in seed layer and with occasional epitaxial growth on seed layer. © 2002 American Institute of Physics. [DOI: 10.1063/1.1447533]

I. INTRODUCTION

Recently Co alloys have also been proposed for 1 terabit/in.² perpendicular magnetic recording media.¹ To attain such recording density, a sufficiently large anisotropy constant (K_u) is critical for the small stable grains. To achieve large K_u , it is important to have good *c*-axis orientation of the Co-alloy thin film. The use of a seed layer for the recording layer is important to control the texture, microstructure, and morphology of the recording layer.² It has been reported that a Ti seed layer enhances the *c*-axis alignment perpendicular to the film plane showing the best magnetic and structural properties in the Co based perpendicular recording media.^{3,4} Good perpendicular magnetic properties have also been reported for Co alloys deposited on 50-nm-thick Ti seed layer.⁵ However, the underlying mechanism of the improvement of the *c*-axis alignment in perpendicular recording media with a thin seed layer is largely unknown.

This article presents a systematic study of the effect of seed layers on the texture and properties of Co based perpendicular recording media and also describes the underlying mechanism for the improvement of *c*-axis alignment in that type of media with a thin seed layer.

II. EXPERIMENTAL DETAILS

CoCrPt thin films were deposited by rf diode sputtering onto naturally oxidized Si (111) wafers at ambient temperature. By using a Tracor x-ray (Spectrace 5000), the film composition was determined to be Co₇₂Cr₁₃Pt₁₅. Ti and Ta were used as seed layers. The Ar sputtering gas pressure was 5 mTorr and the base pressure was below 5×10^{-7} Torr. Co alloy and Ti sputtering rate was 0.1 nm/s and Ta sputtering

rate was 0.09 nm/s. The CoCrPt layer thickness was fixed at 30 nm while seed layer thickness varied from 3 to 100 nm.

The structure of the films was studied with traditional $\theta/2\theta$ scans, in-plane scans and ω scans (rocking curve). In-plane scans and ω scan were performed by a Philips X-pert Pro x-ray diffractometer. A JEOL JEM 2000-EXII and a PHILIPS TECNAI F20 were used to study the microstructure of the films.

III. RESULTS AND DISCUSSION

Traditional $\theta/2\theta$ scans and ω scans were performed on two sets of deposited films to check the texture and *c*-axis alignment of the films. The 0002 CoCrPt peak intensity from traditional $\theta/2\theta$ scan and full width at half maximum (FWHM) of rocking curve from ω scans are plotted against seed layer thickness as shown in Fig. 1. As expected, the peak intensity plots are always out of phase with FWHM plots. That means one can get lower FWHM and higher peak intensity for better texture and *c*-axis alignment and vice versa. For very thin seed layer thickness (3 nm), *c*-axis alignment is weak. The texture is best for a seed layer thickness of 5–10 nm (5 nm for Ti seed layer and 10 nm for Ta seed layer) after which it then deteriorates with the seed layer thickness. The texture and *c*-axis alignment again improve around the seed layer thickness of 40 nm. Beyond this range, the texture deteriorates almost linearly with seed layer thickness. From Fig. 1, it can be seen that one can have the best texture for 5–10 nm seed layer thickness and the second best texture around 40 nm of seed layer thickness. The minimum $\Delta\theta_{50}$ of 5.7 and 4.5 were obtained for 5 nm Ti and 10 nm Ta seed layer thickness, respectively.

The poor 0001 texture of the magnetic layer for very thin seed layer is probably due to the fact that the very thin seed layer cannot wet the substrate perfectly and cannot prevent adsorbed impurities in the magnetic layer.³ To ascertain the

^{a)}Electronic mail: agroy@ece.cmu.edu

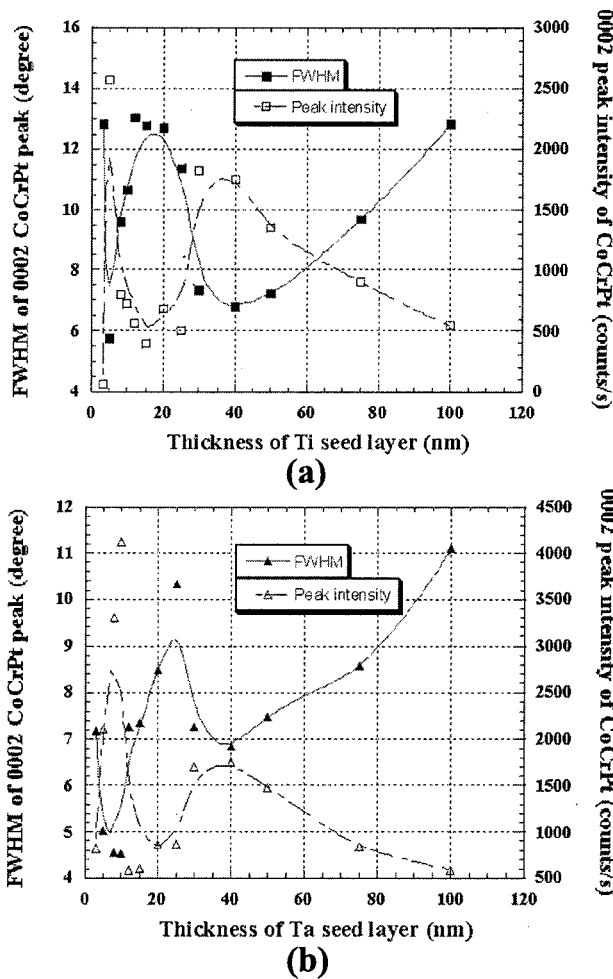


FIG. 1. Dependence of FWHM and peak intensity of 0002 CoCrPt peak with seed layer thickness: (a) Ti and (b) Ta.

mechanism of improvement and deterioration of the *c*-axis alignment of magnetic layer, transmission electron microscopy (TEM) was employed. Figure 2 shows typical plan-view bright field images and corresponding diffraction patterns for different Ti [Figs. 2(a) and 2(b)] and Ta [Figs. 2(c) and 2(d)] seed layer thickness. For Ti 5 nm [Fig. 2(a)] and Ta 10 nm [Fig. 2(c)], images show amorphous microstructure and corresponding electron diffraction patterns show amorphous rings. Whereas, the images and corresponding electron diffraction (ED) patterns of Ti 15 nm [Fig. 2(b)] and Ta 25 nm [Fig. 2(d)] show the microstructure of crystalline and amorphous mixture phases. The microstructure implies that when the seed layers completely wet the substrate and are in amorphous state, it helps to grow natural texture of the magnetic layer. On the other hand, when the film begins to crystallize, the mixture phase disturbs the natural growth of magnetic layer. That is why best and worst texture was observed when the films are in amorphous and mixed phase, respectively.

Figure 3 shows typical in-plane x-ray diffraction (XRD) profiles for different Ti and Ta films. This type of XRD scan probes (*hkl*) planes with normals in the plane of the sample. The profile for 40-nm-thick Ti film [Fig. 3(a)] shows only the (10 $\bar{1}$ 0) peak and no (0002) peak, which implies that it has a

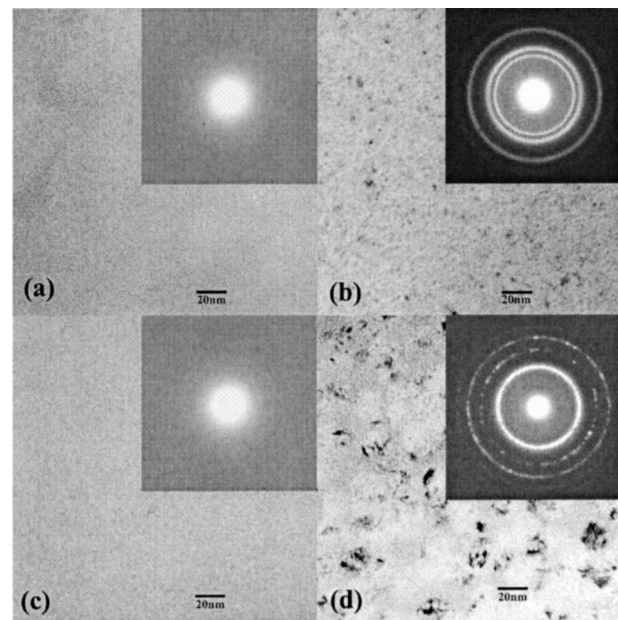


FIG. 2. Typical bright field TEM micrographs and ED patterns of Ti and Ta films: (a) 5 nm Ti, (b) 15 nm Ti, (c) 10 nm Ta and (d) 25 nm Ta.

very good $\langle 0002 \rangle$ fiber texture parallel to the sample normal. The profile for the 100 nm Ti film [Fig. 3(a)] shows a strong (0002) peak along with other peaks implying that the film becomes more random. In Fig. 3(b), the profile for 40 nm Ta shows very weak intensity for (110) while the other profile for 100 nm Ta shows very strong (110) peak with other peaks present. This means 100 nm Ta film becomes random. Whereas, from Fig. 2(d) and from traditional XRD scan (not shown here), one could say that 40 nm Ta promotes a better $\langle 110 \rangle$ fiber texture parallel to the sample normal. Therefore, the improvement of (0002) texture in Ti and (110) texture in Ta for 40-nm-thick-film enhances the *c*-axis alignment in CoCrPt layer. With the thickness increase, the corresponding seed layer texture deteriorates and becomes more random which results in poor *c*-axis alignment in CoCrPt layer.

Cross-sectional TEM was used to examine the growth relationship between seed layer and magnetic layer. Figure 4 shows dark field images for the films deposited on 40 nm Ti [Fig. 4(a)] and 40 nm Ta [Fig. 4(b)] seed layer. It is clear that the bright contrast stretches from seed layer through to magnetic layer in some regions. This implies that there is epitaxial growth of the seed layer and magnetic layer in some grains at that thickness. High-resolution electron microscopy (HRTEM), verifies that occasionally (10 $\bar{1}$ 1) CoCrPt epitaxially grows on (10 $\bar{1}$ 1) Ti, as seen in Fig. 5(a). The epitaxial relationship is (0002)Co/(0002)Ti and $\langle 11\bar{2}0 \rangle$ Co/ $\langle 11\bar{2}0 \rangle$ Ti. The calculated lattice mismatch between Ti (10 $\bar{1}$ 1)//Co(10 $\bar{1}$ 1) is $\sim 18\%$. Figure 5(b) also shows occasional epitaxy between (10 $\bar{1}$ 1) CoCrPt and (101) Ta for 40 nm Ta seed layer film. The lattice mismatch between Ta(110)//Co(10 $\bar{1}$ 1) is $\sim 14\%$. Around 40 nm thickness, the seed layers develop favorable texture which gives rise to (0002) texture in CoCrPt film. Furthermore, the occasional epitaxial growth between seed layer and magnetic layer for

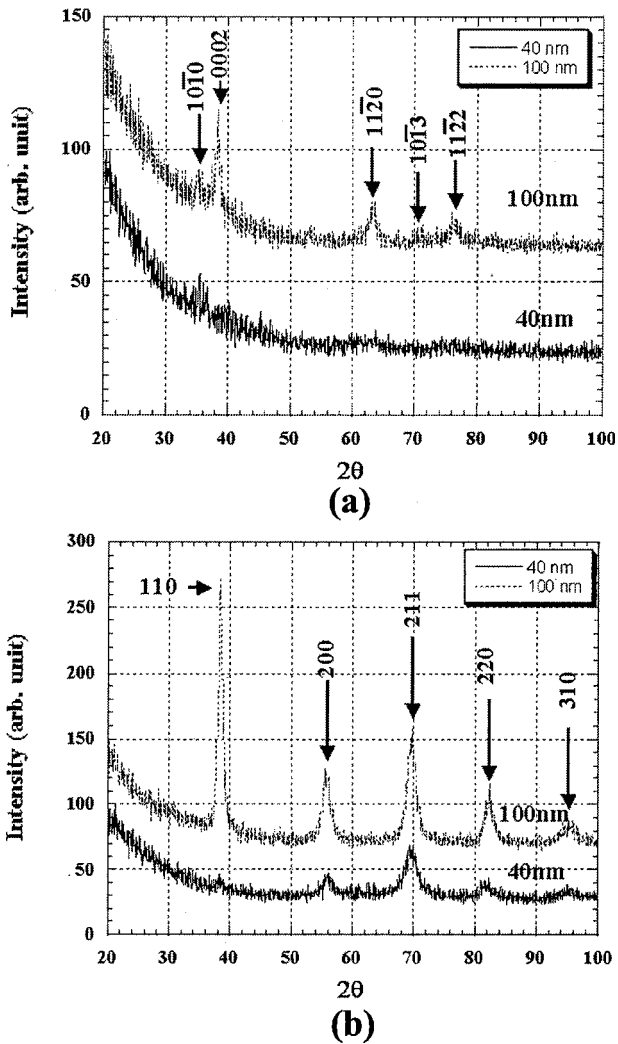


FIG. 3. Typical in-plane XRD scans of Ti (a) and Ta (b) films.

40-nm-thick seed layer films further enhances the *c*-axis alignment in CoCrPt layer. It also appears that Ta enhances better *c*-axis alignment in the magnetic layer than Ti. This is probably due to higher melting point of Ta than Ti. Therefore, Ta stays amorphous for thicker film than Ti and can wet the substrate better.

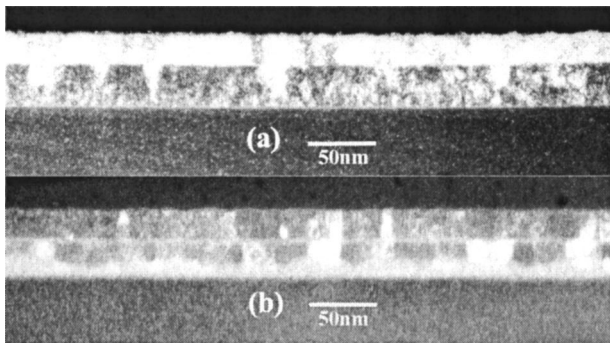


FIG. 4. Cross-sectional TEM dark field images: (a) deposited on 40 nm Ti and (b) deposited on 40 nm Ta.

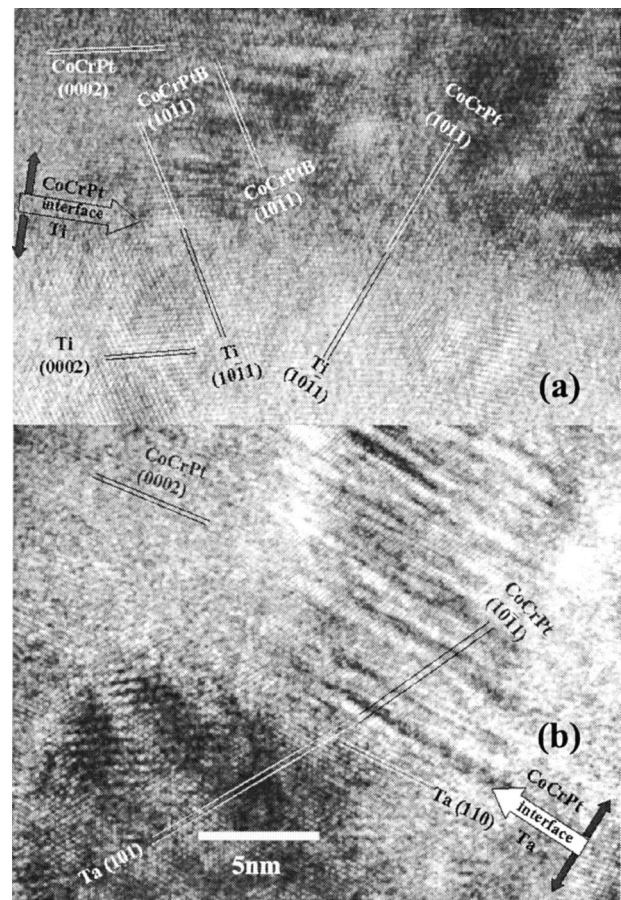


FIG. 5. HRTEM images of interface between seed layer and magnetic layer: (a) deposited on 40 nm Ti and (b) deposited on 40 nm Ta.

IV. CONCLUSIONS

The mechanism of the *c*-axis alignment in Co based perpendicular media with the help of a thin seed layer has been elucidated. Good texture in perpendicular magnetic media can be obtained by two different growth techniques:

- (1) By growing a natural growth texture on amorphous seed layers
- (2) By epitaxial growth of texture on a favorably oriented seed layer. Ta is a better seed layer than Ti to get natural growth texture for perpendicular recording media.

ACKNOWLEDGMENTS

The authors acknowledge the support of Seagate Research, Pittsburgh, PA, through the Data Storage Systems Center and are grateful to N. T. Nuhfer for his assistance in using TECNAI F20.

¹R. Wood, IEEE Trans. Magn. **36**, 36 (2000).

²A. G. Roy, D. E. Laughlin, T. J. Klemmer, K. Howard, S. Khizroev, and D. Litvinov, J. Appl. Phys. **89**, 7531 (2001).

³I. S. Lee, H. Ryu, H. J. Lee, and T. D. Lee, J. Appl. Phys. **85**, 6133 (1999).

⁴T. Shimatsu, H. Komagome, I. Watanabe, H. Muraoka, Y. Sugita, and Y. Nakamura, J. Appl. Phys. **87**, 6367 (2000).

⁵H. Gong, M. Rao, D. E. Laughlin, and D. N. Lambeth, J. Appl. Phys. **85**, 4699 (1999).